BIO HEAT TRANSFER MODEL FOR CLINICAL DERMATOLOGICAL TREATMENT

A THESIS SUBMITTED IN PARTIL FULFILLMENT OF
THE REQUIREMENT FOR THE DEGREE OF

MASTER OF TECHNOLOGY
IN
MECHANICAL ENGINEERING
[Specialization: Thermal Engineering]

By

ALOK AGRAWAL
Roll No. 207ME312

Department of Mechanical Engineering
NATIONAL INSTITUTE OF TECHNOLOGY
ROURKELA
MAY - 2009

BIO HEAT TRANSFER MODEL FOR CLINICAL DERMATOLOGICAL TREATMENT

A THESIS SUBMITTED IN PARTIL FULFILLMENT OF
THE REQUIREMENT FOR THE DEGREE OF

MASTER OF TECHNOLOGY
IN
MECHANICAL ENGINEERING
[Specialization: Thermal Engineering]

By

ALOK AGRAWAL
Roll No. 207ME312

Under the guidance of
Prof. PRASENJIT RATH

Department of Mechanical Engineering
NATIONAL INSTITUTE OF TECHNOLOGY
ROURKELA
May – 2009

National Institute of Technology

Rourkela

C E R T I F I C A T E

This is to certify that the work in this project report entitled **Bio Heat Transfer Model for Clinical Dermatological Treatment** by **Alok Agrawal** has been carried out under my supervision in partial fulfillment of the requirements for the degree of **Master of Technology** in *Mechanical Engineering* with *Thermal Engineering* specialization during session 2008 - 2009 in the Department of Mechanical Engineering, National Institute of Technology, Rourkela.

To the best of our knowledge, this work has not been submitted to any other University/Institute for the award of any degree or diploma.

Dr. Prasenjit Rath
(Supervisor)
Asst. Professor
Dept. of Mechanical Engineering
National Institute of Technology,
Rourkela - 769008

Dedicated to -

Shri L. N. Agrawal

Smt. C. K. Agrawal

my parents for their love
and blessings

Mr. Atul Agrawal

Mrs. Sapna Agrawal

Mrs. Shweta Agrawal

my elder brother and sisters for
their supports

ACKNOWLEDGEMENTS

After the completion of this Thesis, I experience feeling of achievement and satisfaction. Looking into the past I realize how impossible it was for me to succeed on my own. I wish to express my deep gratitude to all those who extended their helping hands towards me in various ways during my short tenure at NIT Rourkela.

I avail this opportunity to express my hereby indebtedness, deep gratitude and sincere thanks to my guide, Prof. P. Rath, Assistant Professor, Mechanical Engineering Department , NIT Rourkela for his in depth supervision and guidance, constant encouragement and co-operative attitude for bringing out this thesis work.

I extend my sincere thanks to Dr. R.K. Sahoo, Professor and Head of Department, Mechanical Engineering Department, NIT Rourkela for his valuable suggestion for bringing out this thesis in time.

I would like to acknowledge the support of every individual who assisted me in making this project a success and I would like to thank Mr. B. N. Padhi, Research Scholar, NIT Rourkela for his help whenever it was required.

Alok Agrawal

May, 2009 NIT Rourkela

Abstract

In traditional engineering studies, the transient term of radiative transfer equation (RTE) can be neglected. This assumption does not lead to important errors since the temporal variations of the observables (e.g. temperature) are slow as compared to the time-of-flight of a photon. However, in many new applications such as pulsed laser interaction with materials, the transient effect must be considered in the RTE. In the transient phase, the reflected and transmitted signals have temporal signatures that persist for a time period greater than the duration of the source pulse. This could be a source of information about the properties field inside the medium. Hence, sufficiently accurate solution methods are required. Predicted signals are dependent on the considered models. The results vary significantly from approximate models.

In the last two decade, finite volume method (FVM) emerged as one of the most attractive method for modeling steady as well as transient state radiative transfer. The finite volume method is a method for representing and evaluating partial differential equations as algebraic equations. Similar to the finite difference method, values are calculated at discrete places on a meshed geometry. "Finite volume" refers to the small volume surrounding each node point on a mesh. In the finite volume method, volume integrals in a partial differential equation that contain a divergence term are converted to surface integral using divergence theorem. These terms are then evaluated as fluxes at the surfaces of each finite volume. Because the flux entering a given volume is identical to that leaving the adjacent volume, these methods are conservative.

The present research work deals with the analysis of transient radiative transfer in one and two-dimensional using FVM. Isothermal absorbing-emitting medium is considered. The two scheme namely Step and CLAM are used to get the value of nodal intensity. The effect of wall emissivity, scattering albedo, optical thickness and phase function on the temporal variation of flux has also been observed. The effect of anisotropic scattering for one-dimensional case has also been studied.

Contents

List of Figures

Nomenclature

a	coefficient of discretization equation
b	source term in discretization equation
c	the speed of light
D'_{cx}, D'_{cy}	direction cosine in x , y direction respectively
G	incident radiation
I	actual intensity
M	total number of control angels
$\hat{n}$	unit outward normal vector of the control volume face
q	heat flux
s	distance
S	source function
S_m^l	modified source function
$S_{ce^+}, S_{cw^+}, S_{cn^+}, S_{cs^+}$	additional source term for high order resolution scheme
$S_{pe^+}, S_{pw^+}, S_{pn^+}, S_{ps^+}$	additional source term for high order resolution scheme
$\hat{s}$	unit direction vector
T	temperature
t	time
x, y, z	coordinate direction
β	extinction coefficient
β_m^l	modified extinction cooefficient

ΔA	area of control volume faces
Δv	volume of control volume
$\Delta x, \Delta y$	x and y direction control volume width
$\Delta\Omega$	control angle
ε	emissivity
θ	polar angle measured from $\hat{e}_z$
κ	absorption coefficient
σ_s	scattering coefficient or Stefan Boltzmann constant
Φ	scattering phase function
$\Phi^{l'l}$	average scattering phase function
ϕ	azimuthal angle measured from $\hat{e}_x$

Subscripts

b	black body
D	downstream
m	modified
P	node
U	upstream
E, W, N, S	east, west, north, south neighbors of P
e, w, n, s	east, west, north, south direction

superscripts

l, l'	angular directions
0	value from previous iteration
*	non-dimensional quantities

CHAPTER 1

INTRODUCTION

1.1 Introduction

Radiative heat transfer is an important mode in high-temperature systems. Thermal radiation is important in many applications, and its analysis is difficult in the presence of a participating medium because of absorption, emission, and scattering. Thermal radiation being electromagnetic waves, it propagates at the speed of light. In most traditional engineering applications, such as in the thermal analysis of boilers, furnaces, internal combustion engines, etc., as temporal variations in thermal quantities of interest are much slower than the time scale associated with the propagation of thermal radiation, the transient term from the radiative transfer equation is neglected, i.e., radiation is assumed to be an instantaneous (steady-state) process.

Rapid progress in technology is making possible to create and observe thermophysical phenomena on increasingly shorter time scale. One such phenomenon of interest is the interaction of pulsed light with participating media.

The recent research on the propagation of ultra-short light pulse inside the absorbing and scattering media has lead to some interesting applications in the area of material properties diagnostic, optical imaging, remote sensing, etc. The time scales of such processes are usually in the order of 10^{-12} to 10^{-15} seconds. In the case of remote sensing using short light pulse, the pulse width is in the order of 10^{-9} seconds. The corresponding spatial and temporal variations of radiation intensity in these processes are comparable. Therefore, the consideration of the transient term in the radiation transport equation is necessary. The simulation of transient radiation process is more complex than that in the steady state due to the hyperbolic wave equation coupled with the in scattering integral term.

In the situations of dealing with extremely short time response to radiation and extremely high rate of change of radiation, the steady-state radiative transfer equation could not provide accurate representations.

The motivation of the current study is to gain a fundamental understanding the unique features of transient radiation and its interaction with the participating medium.

1.2 Literature review

For the last few decades, there is an exponential growth in the research area of transient radiative heat transfer with the interaction of short pulse laser in participating media. Traditional analysis of radiation transfer neglects the transient effect of light propagation due to the large speed of light compared to the local time and length scales [2].

As the technology advanced and the ultra-short pulsed lasers application developed, the steady state assumption is no longer valid as the temporal width of the input pulse is similar to the order of pico and femto-seconds. Ultra-short pulsed lasers are used in a wide variety of applications such as thin film property measurements, micro-machining, removal of contamination particles, ablation of polymers, remote sensing of the atmosphere, combustion chambers and other environments which involve interaction of the laser beam with scattering and absorbing particles of different sizes [3]. Another interesting application of short-pulsed lasers is in optical tomography where their use can potentially provide physiological and morphological information about the interior of living tissues and organs in a non-intrusive manner. All these applications need models to predict transient radiation transport in participating media. In the past, various analytical studies and numerical models of transient radiative transfer have been reviewed by Mitra and Kumar [4]. The normal-mode-expansion technique is used in [1] to obtain a semi-analytical solution for the angular distribution of radiation at any optical distance within a linearly anisotropic scattering, absorbing, emitting, non-isothermal, gray medium between two parallel reflecting boundaries. From the literature it is evident that many researchers adopted different methods to deal with the problem. The commonly used methods to solve the transient radiative transfer equation are the Monte Carlo method, the integral equation solution, the finite volume method (FVM), the radiation element method (REM), discrete transfer method (DTM) and the discrete ordinates method (DOM).

The Monte Carlo method is used to simulate problems involving radiative heat transfer because of its simplicity, the ease by which it can be applied to arbitrary configurations and its ability to capture actual and often complex physical conditions [5]. The Monte Carlo technique has been used by Guo et al. [5] to simulate short-pulsed laser transport in anisotropically scattering and absorbing media. The authors examined the effects of pulse

width, medium properties, and the effects of Fresnel reflection on the transmissivity and reflectivity of the medium. However, the method has inherent statistical errors due to its stochastic nature [2]. It also demands a lot of computational time and computer memory as the histories of the photons have to be stored at every instant of time [5]. Thus, the Monte-Carlo method is ruled out in practical utilizations such as real-time clinical diagnostics where computational efficiency and accuracy are major concerns [6]. Guo and Maruyama [7] evaluated the isotropic law in three dimensional inhomogeneous and linear anisotropic scattering media. The discrete ordinates method has been used by various researchers to solve the transient radiative transfer equation (RTE). Sakami et al. [8] used the DOM with high order upwind piecewise parabolic interpolation scheme to analyze the ultra-short light pulse propagation in an anisotropically scattering two dimensional medium. The upwind difference scheme is needed to resolve the propogation wave front. Mitra et al [9] used a P_1 approximation to model transient radiative transfer in a rectangular enclosure.

Hsu [10] considered the Monte Carlo simulations for transient radiative transfer process within the participating media inside the one-dimensional geometry with the multiple scattering and reflective boundaries. Various effects, including the scattering albedo, pulse shape and width, surface reflectivity and optical thickness, are examined and concluded that if the boundary surface is reflective, then the temporal spread is influenced by multiple reflections and partial transmissions at the surfaces. The backward or reverse Monte Carlo method was successfully applied by Lu and Hsu [11] to simulate transient radiative transport in a non-emitting, absorbing, and anisotropically scattering one-dimensional slab subjected to ultra-short light pulse irradiation. Wu and Coworkers [12] and Tan and Hsu [13] have used the integral equation formulation to solve the transient radiative transfer problem analytically. Tan and Hsu [13] used the integral equation formulation and the radiation element method by Guo and Kumar [14] to simulate radiative transport in the same problem with black boundaries exposed to diffuse or collimated irradiation.

Y.Hasegawa, et al., [15] used Monte Carlo method to simulate the transient light transmission through the living tissue which was characterized by strong forward scattering phase function. Brewster and Yamada [16] later conducted the transient study using the same MC algorithm used by Hasegawa, et al. They examined various effects i.e., albedo, optical thickness, anisotropic scattering, and the detector size, on the reflected and transmitted

temporal signals. Finite volume methods developed by Chai et al., [17] to solve the steady-state RTE have also been employed to solve the transient RTE by Chai [18,19]. The finite volume technique is used with the step and curved line advection method (CLAM) [20] spatial discretization schemes to model transient radiative transfer in 1-D and 2-D geometries. It is found that the FVM procedure gives the complete flexibility in laying out the spatial and angular grids that best capture the physics of the given problem. It is also seen that the step scheme is unable to capture the sharp change in the incident radiation and the radiative flux when the slab is subjected to a continuous collimated incident radiation. When a finite-pulse collimated radiation beam is modeled, the step scheme overpredict the lower limit and underpredict the upper limit of the incident radiation and the radiative flux. The author found that the CLAM scheme captures the penetration depths of radiation more accurately than the step scheme for the same grid.

Rath et al., [21] extended the DTM, to solve transient radiative transport problems in a one-dimensional planar absorbing and scattering medium, one boundary of which is subjected to a short-pulse laser and the other boundary is cold. Effects of optical thickness, scattering albedo, and anisotropy factor on transmittance and reflectance are analyzed. Sarma et al., [22] analyzed the radiative heat transfer problem in 1-D planar absorbing, emitting and anisotropically scattering gray medium in radiative equilibrium subjected to collimated radiation by the discrete transfer method. The Galerkin method is extended by T. Okutucu; Y. Yener [23] for the solution of the transient radiative transfer problem in a one-dimensional participating plane-parallel grey medium with a collimated short-pulse Gaussian irradiation on one of its boundaries. The transient transmittance and reflectance of the medium are evaluated for various optical thicknesses, scattering albedos and pulse durations. Muthukumaran and Mishra [24] used the finite volume method for solving transient radiative heat transfer problem in a planar participating medium subjected to a short-pulse diffuse or collimated radiation. For a train of pulses, effects of the extinction coefficient and the scattering albedo on transmittance and reflectance signals are studied.

A finite element model, which is based on the discrete ordinates method and least-squares variational principle, is developed by W.An et al., [25] to simulate the transient radiative transfer in absorbing and scattering media in one dimensional and two-dimensional enclosure and W.An et al., [26] extended the same method to simulate short-pulse light

radiative transfer in homogeneous and nonhomogeneous media. Their results indicated that the reflected signals can imply the break of optical properties profile and their location. Most recently Yilmazer A, Kocar C [27] discussed the radiative transfer problem in plane-parallel, participating medium with linearly anisotropic scattering using the ultraspherical-polynomials approximation method. Effects of the order of approximation, optical thickness, specular reflection, anisotropic scattering, and change of the source term on results are investigated different order of approximation.

Majority of the findings are based on the most simplified assumption of black wall, whereas the reflective wall assumption resembles more to the practical application [4]. The multiple scattering and reflective boundaries, influences considerably the radiation transport in a participating medium. When the boundary surface becomes reflective, then the temporal spread changes significantly by the multiple reflections and partial transmissions at the surfaces [10]. Therefore, the present article focuses on the problem of a plane-parallel participating medium bounded by diffusely emitting boundaries, under the condition of radiative equilibrium. The total intensity is directly solved using FVM without splitting into the collimated part and diffusive part as cited in existing formulation [21, 22, 24, 28].

1.3 Objective of Present work

- ✓ To gain a fundamental understanding and unique features of transient radiation.
- ✓ Behavior of Transient Radiation in the participating medium is to be study. (Absorbing, emitting and scattering medium)
- ✓ Finite Volume Formulation of Radiative Heat Transfer in both 1-D and 2-D model including effect of anisotropic scattering in 1-D model.
- ✓ Use of two different schemes to do above formulation i.e. Step and CLAM and compare the result that which is giving better result.
- ✓ To study the effect of various parameter of RTE on wall flux.

CHAPTER 2

MATHEMATICAL FORMULATION

In this chapter , the problem formulation is describe in detail. The finite volume method is used to discretize the governing TRT equation. Two spatial differencing scheme namely the STEP and the CLAM are used to discretize the spatial derivative term in the TRTE.

This chapter is divided into three sections. In section 2.1, formulation for 1-D model is described. In section 2.2 formulations for 2-D is described. Formulation for 1-D model with anisotropic scattering is described in section 2.3.

2.1 1-D Model

The computational domain for the 1-D problem is shown in Fig (2.1), the medium is isothermal emitting-absorbing maintained at constant temperature with both walls are maintained cold.

The Transient Radiative Transfer Equation for 1-D problem is given as follows

Transient Radiative Transfer Equation (TRTE)

The TRTE for a gray medium can be written as

$$\frac{1}{c}\frac{\partial I(r,\hat{s},t)}{\partial t}+\frac{\partial I(r,\hat{s},t)}{\partial s}=-k(r)I(r,\hat{s},t)-\sigma_s(r)I(r,\hat{s},t)+k(r)I_b+\frac{\sigma_s(r)}{4\pi}\int_{4\pi}I(r,\hat{s}',t)\phi(r,\hat{s}',\hat{s},t)d\Omega' \quad (1)$$

where c = ds/dt is the speed with which the radiation intensity propagates.

$$\frac{1}{c}\frac{\partial I(r,\hat{s},t)}{\partial t}+\frac{\partial I(r,\hat{s},t)}{\partial s}=-\beta I(r,\hat{s},t)+k(r)I_b+\frac{\sigma_s(r)}{4\pi}\int_{4\pi}I(r,\hat{s},t)\phi(r,\hat{s}',\hat{s},t)d\Omega' \quad (2)$$

which can be further reduced to

$$\frac{1}{c}\frac{\partial I(r,\hat{s},t)}{\partial t}+\frac{\partial I(r,\hat{s},t)}{\partial s}=-\beta I(r,\hat{s},t)+S(r,\hat{s},t) \tag{3}$$

where extinction coefficient, $\beta = k(r)+\sigma_s(r)$ (4)

and source function, $S(r,\hat{s},t)=k(r)I_b+\frac{\sigma_s(r)}{4\pi}\int_{4\pi} I(r,\hat{s}',t)\phi(r,\hat{s}',\hat{s},t)d\Omega'$ (5)

where the terms on the left hand side represents radiation intensity gradient with respect to time and space. On the right hand side, the first term indicates the attenuation of radiation intensity due to absorption in the direction of travel and out scattering from the direction of travel. The total attenuation of radiant energy depends on two factors. These are (1) the relative importance of absorption and scattering and (2) the total "strength" of absorption and scattering. The first factor is described by the scattering albedo, ω.

This factor is defined as

$$\omega=\frac{\sigma_s}{k+\sigma_s} \tag{6}$$

From Eq. (6), scattering albedo for a purely absorbing medium is ω = 0, while ω is unity for purely scattering medium.

The second factor is described by the optical thickness. It is defined as

$$\tau=(k+\sigma_s)L_c \tag{7}$$

Where L_c is the representative characteristic length of the problem considered.

The second and third term represent the augmentation part due to emission from the medium and in scattering from all other directions. The total augmentations of the radiant energy depend upon the scattering phase functions.

The boundary condition for the present problem for an opaque diffuse surface is as follows

Boundary condition for an opaque diffuse surface.

The radiation energy leaving the opaque diffuse surface consists of two components. These are the emission due to the temperature of the surface and reflection of the incoming intensities. Mathematically, this can be written as

$$I(r,\hat{s},t) = \varepsilon(r) I_b(r,t) + \frac{1-\varepsilon(r)}{\pi} \int_{\hat{s}'.\hat{n}<0} I(r,\hat{s}',t)\left|\hat{s}'.\hat{n}\right| d\Omega' \tag{8}$$

Equation (8) provides the boundary intensity for the TRTE

The probability that a ray from one direction will be scattered into certain other direction will be described by scattering phase function which is further describe as follows

Scattering phase function

The scattering phase function ϕ in the TRTE describes how radiation energy is scattered in a participating medium. Scattering can be classified into two categories. These are isotropic and anisotropic scattering. Isotropic scattering indicates energy scattered equally in all the directions whereas anisotropic scattering can be forward and backward scattering. Scattering phase function should satisfy

$$\int_{4\pi} \phi(\hat{s}',\hat{s}) d\Omega' = 4\pi \tag{9}$$

The phase function is a measure of the anisotropy of the scattering. It provides a factor for each direction with which the incoming intensity has to be multiplied to give the outgoing intensity. Hence, for isotropic scattering, the phase function is 1 for all directions.

The Radiative heat transfer relations i.e. irradiation and radiative heat flux is defined as

Radiation heat transfer relations

The incident radiation is defined as

$$G(r,t) = \int I(r,\hat{s},t)d\Omega \tag{10}$$

The radiative heat flux in direction i is defined as

$$q_i = \int_{2\pi} I(r,\hat{s},t)(\hat{s},\hat{i})d\Omega \tag{11}$$

where $\hat{i}$ is the unit vector pointing in the i direction direction.

The divergence of the radiative heat flux is

$$\nabla.q = k\left[4\pi I_b(r,t) - G(r,t)\right] \tag{12}$$

In combined mode of heat transfer as well as in radiation dominated process, the divergence of radiative heat flux plays a vital role. In the absence of a heat source/sink, a system is in radiative equilibrium if other modes of heat transfer are negligible. Under such conditions $\nabla.q = 0$ and the temperature of the medium can be obtained from equation (12).

The formulations for 1-D problem are as follows

Formulation of the Discretization equation

The discretization equation can be obtained by integrating the TRTE over typical control volume, a control angle and for a small interval of time.

For a particular control angle l, the equation (1) can be written as

$$\frac{1}{c}\frac{\partial I^{l}}{\partial t}+\frac{\partial I^{l}}{\partial s}=-\beta I^{l}+kI_{b}+\frac{\sigma_{s}}{4\pi}\sum_{l'=l}^{M}I^{l}\Phi^{l'l}\Delta\Omega^{l'}=-\left(\beta-\frac{\sigma_{s}}{4\pi}\Phi^{ll}\Delta\Omega^{l}\right)I^{l}+$$
$$kI_{b}+\frac{\sigma_{s}}{4\pi}\sum_{\substack{l'=1\\l'\neq l}}^{M}I^{l'}\Phi^{l'l}\Delta\Omega^{l} \qquad (13)$$

where $I^{l}=I(r,\hat{s},t)$. The inscattering term is summed over all the control angles used to discretize the domain under construction.

Now the linearised TRTE can be written as

$$\frac{1}{c}\frac{\partial I^{l}}{\partial t}+\frac{\partial I}{\partial s}=-\beta_{m}^{l}I^{l}+S_{m}^{l} \qquad (14)$$

where modified extinction coefficient, $\beta_{m}^{l}=\left(\beta-\frac{\sigma_{s}}{4\pi}\Phi^{ll}\Delta\Omega^{l}\right)$ (15)

and modified source function, $S_{m}^{l}=kI_{b}+\frac{\sigma_{s}}{4\pi}\sum_{\substack{l'=1\\l'\neq l}}^{M}I^{l'}\Phi^{l'l}\Delta\Omega^{l'}$ (16)

Upon integration over a typical two dimensional control volume and a control angle within a specified time step, the TRTE becomes

$$\int_{\Delta\Omega'}\int_{\Delta V}\int_{\Delta t}\frac{1}{c}\frac{\partial I^{l}}{\partial t}dtdvd\Omega+\int_{\Delta\Omega'}\int_{\Delta V}\int_{\Delta t}\frac{\partial I^{l}}{\partial s}dtdvd\Omega=\int_{\Delta\Omega'}\int_{\Delta V}\int_{\Delta t}\left(-\beta_{m}^{l}+S_{m}^{l}\right)dtdvd\Omega \qquad (17)$$

Applying divergence theorem to the 2nd term of the equation (17), the TRTE simplifies to

$$\int_{\Delta\Omega'}\int_{\Delta V}\int_{\Delta t}\frac{1}{c}\frac{\partial I^l}{\partial t}dtdvd\Omega+\int_{\Delta\Omega'}\int_{\Delta V}\int_{\Delta A}I^l\left(s^l.\hat{n}\right)dtdAd\Omega=\int_{\Delta\Omega'}\int_{\Delta V}\int_{\Delta t}\left(-\beta_m^l I^l+S_m^l\right)dtdvd\Omega \tag{18}$$

where $\hat{n}$ is the unit outward normal vector. The first term in the left hand side represents the change of radiation intensity with time; the second term represents the inflow and outflow of radiant energy across the faces of the control volume. The term on the right side accounts for the attenuation and augmentation of energy within a control volume and control angle. In the finite volume method, the magnitude of intensity is assumed to be constant over the control volume and a control angle. Under these assumptions and using the fully implicit scheme, the equation (18) can be written as

$$\frac{1}{c}\left(I_p^l-I_p^{l0}\right)\Delta V\Delta\Omega^l+\sum_{i=1}^{2}I_i^l\Delta A_i\Delta t\int_{\Delta\Omega'}\left(\hat{s},\hat{n}\right)d\Omega'=\left(-\beta_{m,p}^l I_p^l+S_{m,p}^l\right)\Delta V\Delta\Omega^l\Delta t \tag{19}$$

Where I_P^{l0} and I_P^l are the nodal intensities at the start and at the end of the time step respectively. On further simplification, for a control volume and a control angle the equation (19) becomes

$$\frac{1}{c}\left(I_p^l-I_p^{l0}\right)\Delta V\Delta\Omega^l+\left(I_n^l-I_s^l\right)\Delta A_y D_{cy}^l\Delta t=\left(-\beta_{m,p}^l I_p^l+S_{m,p}^l\right)\Delta V\Delta\Omega^l\Delta t \tag{20}$$

Where $D_{cyn}^l=\int\left(\hat{s}.\hat{n}_y\right)d\Omega^l=-D_{cys}^l=D_{cy}^l$

$$\Delta\Omega^l=\int_{\Delta\Omega'}d\Omega$$

$$\Delta A_{xn}=\Delta A_{xs}$$

To relate the boundary intensities to the nodal intensities, two spatial difference scheme: STEP, CLAM are used. In the step or upwind scheme the downstream boundary intensities are set equal to the upstream nodal intensities.

$$I_n^l = I_P^l, \quad I_s^l = I_S^l, \tag{21}$$

Applying the STEP scheme, eq^n (20) becomes,

$$\left[D_{cy}^l + \beta_{m,p}^l \Delta V \Delta\Omega^l + \frac{\Delta V \Delta\Omega^l}{c\Delta t} \right] I_p^l = \left(\frac{\Delta V \Delta\Omega^l}{c\Delta t} \right) I_P^{l0} + D_{cy}^l I_S^l + S_{m,P}^l \Delta V \Delta\Omega^l \tag{22}$$

The standard form of the discretisation equation in control volume formulation is

$$a_P I_P = a_P^0 I_P^0 + \sum a_{nb} I_{nb} + b \tag{23}$$

So the final discretisation equation for the nodal intensities for the $D_{cy}^l \rangle 0$ conditions can be written as

$$a_P^l I_P^l = a_P^{l0} I_P^{l0} + a_S^l I_S^l + b^l$$

where

$$a_P^{l0} = \frac{\Delta V \Delta\Omega^l}{c\Delta t} \qquad a_S^l = \Delta x D_{cy}^l$$

$$a_P = \left[\Delta x D_{cy}^l + \beta_{mP}^l \Delta V \Delta\Omega^l + \frac{\Delta V \Delta\Omega^l}{c\Delta t} \right]$$

$$b = S_{mP}^l \Delta V \Delta\Omega^l$$

CLAM Scheme

High order resolution CLAM scheme express the dependent variables (the radiative intensity in the present case) at a cell face f as a function of its values present at three neighboring grid nodes, two upstream and one downstream from the cell face. In this formulation a normalized intensity and a normalized co-ordinate is defined as

$$\tilde{I} = \frac{I - I_U}{I_D - I_U} \tag{24}$$

$$\tilde{x} = \frac{x - x_U}{x_D - x_U} \tag{25}$$

The schematic of control volume and radiation direction in case of 1-D problem is shown in fig (2.2)

At face,

$$\tilde{I}_f = \frac{(\tilde{x}_C^2 - \tilde{x}_f)}{\tilde{x}_C(\tilde{x}_C - 1)}\tilde{I}_C + \frac{(\tilde{x}_f - \tilde{x}_C)}{\tilde{x}_C(\tilde{x}_C - 1)}\tilde{I}_C^2 \qquad \text{for } 0 < \tilde{I}_C < 1 \tag{26}$$

$$\tilde{I}_f = \tilde{I}_C \qquad \text{elsewhere} \tag{27}$$

for north face

$$\tilde{I}_n = \frac{(\tilde{x}_P^2 - \tilde{x}_n)}{\tilde{x}_P(\tilde{x}_P - 1)}\tilde{I}_P + \frac{(\tilde{x}_n - \tilde{x}_P)}{\tilde{x}_P(\tilde{x}_P - 1)}\tilde{I}_C^2 \tag{28}$$

$$I_n = I_P + S_{cn^+} + S_{pn^+} I_P \tag{29}$$

where

$$\tilde{x}_P = \frac{x_P - x_S}{x_N - x_S} = 0.5 \qquad \tilde{x}_n = \frac{x_n - x_S}{x_N - x_S} = 0.75 \tag{30}$$

$$S_{cn^+} = I_N\left(\frac{I_P - I_S}{I_N - I_S}\right) \qquad S_{pn^+} = -\left(\frac{I_P - I_S}{I_N - I_S}\right) \tag{31}$$

For south face,

$$\widetilde{I}_s = \frac{(\widetilde{x}_S^2 - \widetilde{x}_s)}{\widetilde{x}_S(\widetilde{x}_S - 1)}\widetilde{I}_W + \frac{(\widetilde{x}_s - \widetilde{x}_S)}{\widetilde{x}_S(\widetilde{x}_S - 1)}\widetilde{I}_S^2 \tag{32}$$

$$I_s = I_S + S_{cs^+} + S_{ps^+} I_P \tag{33}$$

where

$$\widetilde{x}_S = \frac{x_S - x_{SS}}{x_P - x_{SS}} = 0.5 \qquad \widetilde{x}_s = \frac{x_s - x_{SS}}{x_P - x_{SS}} = 0.75 \tag{34}$$

$$S_{cs^+} = -I_S\left(\frac{I_S - I_{SS}}{I_P - I_{SS}}\right) \qquad S_{ps^+} = \left(\frac{I_S - I_{SS}}{I_P - I_{SS}}\right) \tag{35}$$

Now applying the CLAM scheme, eq^n (20) become,

$$\left[D_{cy}^l(1 + S_{pn^+} - S_{ps^+}) + \beta_{m,P}^l \Delta V \Delta\Omega^l + \frac{\Delta V \Delta\Omega^l}{c\Delta t}\right] I_P^l = \left(\frac{\Delta V \Delta\Omega^l}{c\Delta t}\right) I_P^{l0} + D_{cn}^l I_S^l + D_{cn}^l (S_{cs^+} - S_{cn^+}) + S_{m,P}^l \Delta V \Delta\Omega^l \tag{36}$$

So the final discretisation equation for the nodal intensities for the $D_{cy}^l \rangle 0$ condition can be written as

$$a_P^l I_P^l = a_P^{l0} I_P^{l0} + a_S^l I_S^l + b^l$$

where

$$a_P^{l0} = \frac{\Delta V \Delta\Omega^l}{c\Delta t} \qquad a_S^l = \Delta x D_{cy}^l$$

$$a_P = \left[D_{cy}^l(1 + S_{pn^+} - S_{ps^+}) + \beta_{m,P}^l \Delta V \Delta\Omega^l + \frac{\Delta V \Delta\Omega^l}{c\Delta t}\right]$$

$$b^l = D_{cy}^l (S_{cs^+} - S_{cn^+}) + S_{m,P}^l \Delta V \Delta\Omega^l$$

2.2 2-D Model

The formulation of 2-D model is similar to the 1-D model upto equation (18) with similar boundary condition. After that one more direction added to make the formulation to 2-D. So the equation (18) can be written as

$$\frac{1}{c}\left(I_p^l - I_p^{l0}\right)\Delta V\Delta\Omega^l + \sum_{i=1}^{4} I_i^l \Delta A_i \Delta t \int_{\Delta\Omega'} (\hat{s},\hat{n})d\Omega' = \left(-\beta_{m,p}^l I_p^l + S_{m,p}^l\right)\Delta V\Delta\Omega^l\Delta t \tag{37}$$

where I_P^{l0} and I_P^l are the nodal intensities at the start and at the end of the time step respectively. On further simplification, for a control volume and a control angle the equation (37) becomes

$$\frac{1}{c}\left(I_P^l - I_P^{l0}\right)\Delta V\Delta\Omega^l + \left(I_e^l - I_w^l\right)\Delta A_x D_{cx}^l \Delta t + (I_n^l - I_s^l)\Delta A_y D_{cy}^l \Delta t = \left(-\beta_{m,P}^l I_P^l + S_{m,P}^l\right)\Delta V\Delta\Omega^l\Delta t \tag{38}$$

where $D_{cxe}^l = \int (\hat{s}.\hat{n}_x)d\Omega^l = -D_{cxw}^l \qquad D_{cyn}^l = \int (\hat{s}.\hat{n}_y)d\Omega^l = -D_{cys}^l$

$$\Delta\Omega^l = \int_{\Delta\Omega'} d\Omega$$

$$\Delta A_x = \Delta A_y$$

The computational domain for the 2-D problem considered is shown in fig (2.3)

To relate the boundary intensities to the nodal intensities, two spatial difference scheme: STEP & CLAM are used. In the step or upwind scheme the downstream boundary intensities are set equal to the upstream nodal intensities.

$$I_e^l = I_P^l,\ \ I_w^l = I_W^l,\ \ I_n^l = I_p^l,\ \ I_s^l = I_S^l \tag{39}$$

The schematic of 2-D problem is shown in fig (2.4). The direction of intensity with complete notation is described in that figure. Fig (2.5) and Fig (2.6) shows a typical control angel and intensity in certain direction.

Applying the STEP scheme, eq^{n} (38) becomes,

$$\left[D_{cx}^{l} + D_{cy}^{l} + \beta_{m,P}^{l} \Delta V \Delta\Omega^{l} + \frac{\Delta V \Delta\Omega^{l}}{c\Delta t} \right] I_{P}^{l} = \left(\frac{\Delta V \Delta\Omega^{l}}{c\Delta t} \right) I_{P}^{l0} + D_{cx}^{l} I_{W}^{l} + D_{cy}^{l} I_{S}^{l} + S_{m,P}^{l} \Delta V \Delta\Omega^{l} \tag{40}$$

So the final discretisation equation for the nodal intensities for the $D_{cx}^{l} \rangle 0$ and $D_{cy}^{l} \rangle 0$ conditions can be written as

$$a_{P}^{l} I_{P}^{l} = a_{P}^{l0} I_{P}^{l0} + a_{W}^{l} I_{W}^{l} + a_{S}^{l} I_{S}^{l} + b^{l}$$

where

$$a_{P}^{l0} = \frac{\Delta V \Delta\Omega^{l}}{c\Delta t} \qquad a_{W}^{l} = \Delta y D_{cx}^{l} \qquad a_{S}^{l} = \Delta x D_{cy}^{l}$$

$$a_{P} = \left[\Delta x D_{cy}^{l} + \Delta y D_{cx}^{l} + \beta_{mP}^{l} \Delta V \Delta\Omega^{l} + \frac{\Delta V \Delta\Omega^{l}}{c\Delta t} \right]$$

$$b = S_{mP}^{l} \Delta V \Delta\Omega^{l}$$

Now applying CLAM Scheme for 2-D problem same as applied for 1-D problem with extra two directions.

CLAM Scheme

Here also in this formulation of 2-D a normalized intensity and a normalized co-ordinate is defined as

$$\widetilde{I} = \frac{I - I_U}{I_D - I_U} \tag{41}$$

$$\widetilde{x} = \frac{x - x_U}{x_D - x_U} \tag{42}$$

At face,

$$\widetilde{I}_f = \frac{(\widetilde{x}_C^2 - \widetilde{x}_f)}{\widetilde{x}_C(\widetilde{x}_C - 1)}\widetilde{I}_C + \frac{(\widetilde{x}_f - \widetilde{x}_C)}{\widetilde{x}_C(\widetilde{x}_C - 1)}\widetilde{I}_C^2 \qquad \text{for } 0 < \widetilde{I}_C < 1 \tag{43}$$

$$\widetilde{I}_f = \widetilde{I}_C \qquad \text{elsewhere} \tag{44}$$

For east face

$$\widetilde{I}_e = \frac{(\widetilde{x}_P^2 - \widetilde{x}_e)}{\widetilde{x}_P(\widetilde{x}_P - 1)}\widetilde{I}_P + \frac{(\widetilde{x}_e - \widetilde{x}_P)}{\widetilde{x}_P(\widetilde{x}_P - 1)}\widetilde{I}_C^2 \tag{45}$$

$$I_e = I_P + S_{ce^+} + S_{pe^+} I_P \tag{46}$$

where

$$\widetilde{x}_P = \frac{x_P - x_W}{x_E - x_W} = 0.5 \qquad \widetilde{x}_e = \frac{x_e - x_W}{x_E - x_W} = 0.75 \tag{47}$$

$$S_{ce^+} = I_E\left(\frac{I_P - I_W}{I_E - I_W}\right) \qquad S_{pe^+} = -\left(\frac{I_P - I_W}{I_E - I_W}\right) \tag{48}$$

For west face,

$$\widetilde{I}_w = \frac{(\widetilde{x}_W^2 - \widetilde{x}_w)}{\widetilde{x}_W(\widetilde{x}_W - 1)}\widetilde{I}_W + \frac{(\widetilde{x}_w - \widetilde{x}_W)}{\widetilde{x}_W(\widetilde{x}_W - 1)}\widetilde{I}_W^2 \tag{49}$$

$$I_w = I_W + S_{cw^+} + S_{pw^+} I_P \tag{50}$$

where

$$\widetilde{x}_W = \frac{x_W - x_{WW}}{x_P - x_{WW}} = 0.5 \qquad \widetilde{x}_w = \frac{x_w - x_{WW}}{x_P - x_{WW}} = 0.75 \tag{51}$$

$$S_{cw^+} = -I_W(\frac{I_W - I_{WW}}{I_P - I_{WW}}) \qquad S_{pw^+} = (\frac{I_W - I_{WW}}{I_P - I_{WW}}) \tag{52}$$

Similarly,

For north face

$$\widetilde{I}_n = \frac{(\widetilde{x}_P^2 - \widetilde{x}_n)}{\widetilde{x}_P(\widetilde{x}_P - 1)}\widetilde{I}_P + \frac{(\widetilde{x}_n - \widetilde{x}_P)}{\widetilde{x}_P(\widetilde{x}_P - 1)}\widetilde{I}_C^2 \tag{53}$$

$$I_n = I_P + S_{cn^+} + S_{pn^+} I_P \tag{54}$$

where

$$\widetilde{x}_P = \frac{x_P - x_S}{x_N - x_S} = 0.5 \qquad \widetilde{x}_n = \frac{x_n - x_S}{x_N - x_S} = 0.75 \tag{55}$$

$$S_{cn^+} = I_N(\frac{I_P - I_S}{I_N - I_S}) \qquad S_{pn^+} = -(\frac{I_P - I_S}{I_N - I_S}) \tag{56}$$

For south face,

$$\widetilde{I}_s = \frac{(\widetilde{x}_S^2 - \widetilde{x}_s)}{\widetilde{x}_S(\widetilde{x}_S - 1)}\widetilde{I}_S + \frac{(\widetilde{x}_s - \widetilde{x}_S)}{\widetilde{x}_S(\widetilde{x}_S - 1)}\widetilde{I}_S^2 \tag{57}$$

$$I_s = I_S + S_{cs^+} + S_{ps^+} I_P \tag{58}$$

where

$$\widetilde{x}_S = \frac{x_S - x_{SS}}{x_P - x_{SS}} = 0.5 \qquad \widetilde{x}_s = \frac{x_s - x_{SS}}{x_P - x_{SS}} = 0.75 \tag{59}$$

$$S_{cs^+} = -I_S\left(\frac{I_S - I_{SS}}{I_P - I_{SS}}\right) \qquad S_{ps^+} = \left(\frac{I_S - I_{SS}}{I_P - I_{SS}}\right) \tag{60}$$

Now applying the CLAM scheme, eq (34) become,

$$\left[D^l_{cx}(1 + S_{pe^+} - S_{pw^+}) + D^l_{cy}(1 + S_{pn^+} - S_{ps^+}) + \beta^l_{m,P}\Delta V\Delta\Omega^l + \frac{\Delta V\Delta\Omega^l}{c\Delta t}\right] I^l_P = \left(\frac{\Delta V\Delta\Omega^l}{c\Delta t}\right) I^{l0}_P + D^l_{cx} I^l_W + D^l_{cx}(S_{cw^+} - S_{ce^+}) + D^l_{cy} I^l_S + D^l_{cy}(S_{cs^+} - S_{cn^+}) + S^l_{m,P}\Delta V\Delta\Omega^l \tag{61}$$

So the final discretisation equation for the nodal intensities for the $D^l_{cx} \rangle 0$ and $D^l_{cy} \rangle 0$ conditions can be written as

$$a^l_P I^l_P = a^{l0}_P I^{l0}_P + a^l_W I^l_W + a^l_S I^l_S + b^l$$

where

$$a^{l0}_P = \frac{\Delta V\Delta\Omega^l}{c\Delta t} \qquad a^l_W = \Delta y D^l_{cx} \qquad a^l_S = \Delta x D^l_{cy}$$

$$a_P = \left[D^l_{cx}(1 + S_{pe^+} - S_{pw^+}) + D^l_{cy}(1 + S_{pn^+} - S_{ps^+}) + \beta^l_{m,P}\Delta V\Delta\Omega^l + \frac{\Delta V\Delta\Omega^l}{c\Delta t}\right]$$

$$b^l = D^l_{cx}(S_{cw^+} - S_{ce^+}) + D^l_{cy}(S_{cs^+} - S_{cn^+}) + S^l_{m,P}\Delta V\Delta\Omega^l$$

2.3 1-D Model for Anisotropic scattering

In the previously formulated discretization equation of the transient radiative heat transfer the participating medium was taken to be isotropically emitting, absorbing and scattering. But in reality the participating medium has some anisotropicity involved in it.

The physical case under consideration is a one dimensional anisotropically scattering and absorbing medium of length *L* having azimuthal symmetry and constant properties. The equation of transient radiative transfer in the case considered may be expressed as

$$\frac{1}{c}\frac{\partial I^{l}}{\partial t}+\frac{\partial I^{l}}{\partial s}=-kI^{l}-\sigma_{s}I^{l}+kI_{b}+\frac{\sigma_{s}}{4\pi}\int_{4\pi}I^{l'}\phi\left(l'\rightarrow l\right)d\Omega^{l'} \tag{62}$$

For linear anisotropic scattering the phase function is as follows

$$\phi\left(\hat{s}^{l'}\rightarrow\hat{s}^{l}\right)=1+\cos\theta^{l}\cos\theta^{l'} \tag{63}$$

The radiation intensity leaving a gray surface that emits and reflects energy diffusely, can be written as

$$I^{l}=\varepsilon I_{b}+\frac{1-\varepsilon}{\pi}\int_{\hat{s}'\hat{n}<0}I^{l'}\left|\hat{s}'\hat{n}\right|d\Omega^{l'} \tag{64}$$

Equation (64) provides the boundary intensity for the TRTE

It can be seen that due to addition of anisotropic scattering there is a modification in modified extinction coefficient and modified source function. In this section only that modification has been describe and rest of the formulation is same as described in section 2.1, due to the anisotropic scattering the phase function not remain unity now and has some other value which is describe here.

For a particular control angle *l*, the equation (62) can be written linear anisotropic scattering phase function as

$$\frac{1}{\beta c}\frac{\partial I^l}{\partial t}+\frac{1}{\beta}\frac{\partial I^l}{\partial s}=-I^l+(1-\omega)I_b+\frac{\omega}{4\pi}\sum_{l'=l}^{M}I^l\Phi^{l'l}\Delta\Omega^{l'} \tag{65}$$

$$=\left[\frac{\omega}{4\pi}a\cos\theta^l\cos\theta^{l'}\Delta\Omega^l-\left(1-\frac{\omega}{4\pi}\Delta\Omega^l\right)\right]I^l+$$

$$\left[(1-\omega)I_b+\frac{\omega}{4\pi}\left\{\sum_{\substack{l'=1\\l'\neq l}}^{M}I^{l'}\Delta\Omega^{l'}+a\cos\theta\sum_{\substack{l'=1\\l'\neq l}}^{M}I^{l'}\cos\theta^{l'}\Delta\Omega^{l'}\right\}\right]$$

Now the linearised TRTE can be written as

$$\frac{1}{\beta c}\frac{\partial I^l}{\partial t}+\frac{1}{\beta}\frac{\partial I^l}{\partial s}=\beta_m^l I^l+S_m^l \tag{67}$$

where modified extinction coefficient

$$\beta_m^l=\frac{\omega}{4\pi}a\cos\theta^l\cos\theta^{l'}-\left(1-\frac{\omega}{4\pi}\Delta\Omega^l\right) \tag{68}$$

And modified source function ,

$$S_m^l=(1-\omega)I_b+\left[\frac{\omega}{4\pi}\sum_{\substack{l'=1\\l'\neq l}}^{M}I^{l'}\Delta\Omega^{l'}+a\cos\theta\sum I^{l'}\cos\theta^{l'}\Delta\Omega^{l'}\right] \tag{69}$$

Then the remaining formulation is same as section 2.1 and can be refer from there.

In this chapter the complete formulation of the problem for both 1-D and 2-D has been described using FVM method for both Step and CLAM scheme. The effect of anisotropicity in 1-D model has been described. In the next chapter numerical method will be discussed like overall positive variable treatment, Finite Volume Method and Solution procedure.

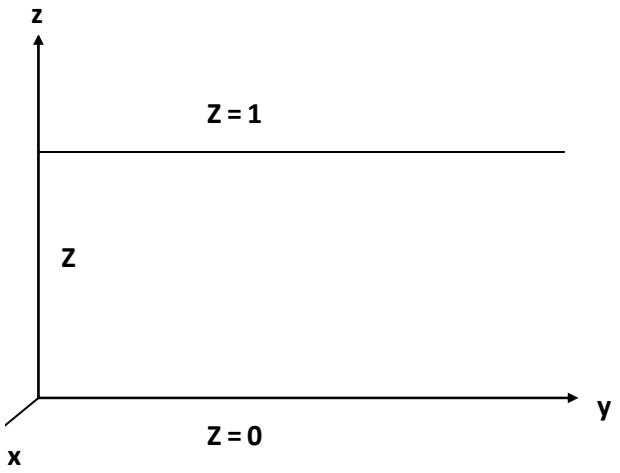

Fig 2.1 a typical 1-D computational domain

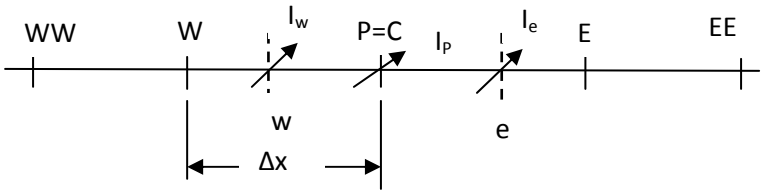

Fig 2.2 control volume and radiation direction for 1-D problem

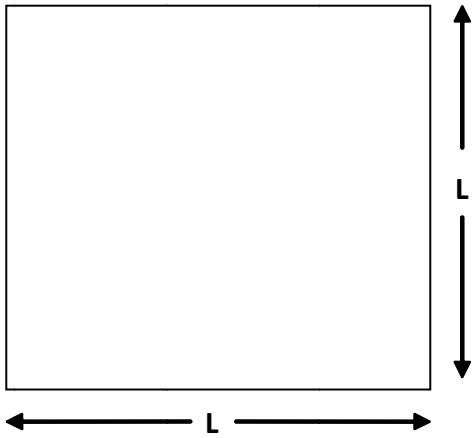

Fig 2.3 A typical 2-D computational domain

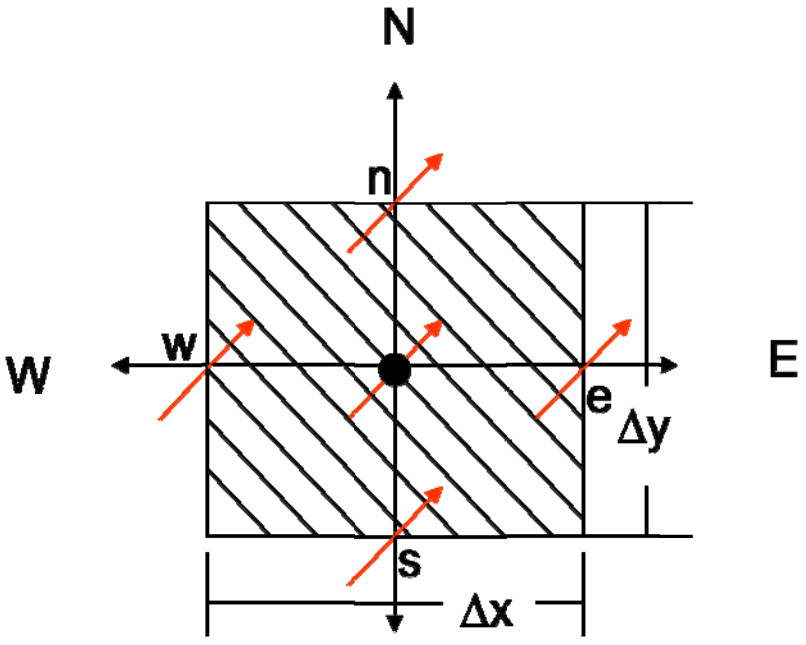

Fig 2.4 A typical control volume for 2-D with specified notations

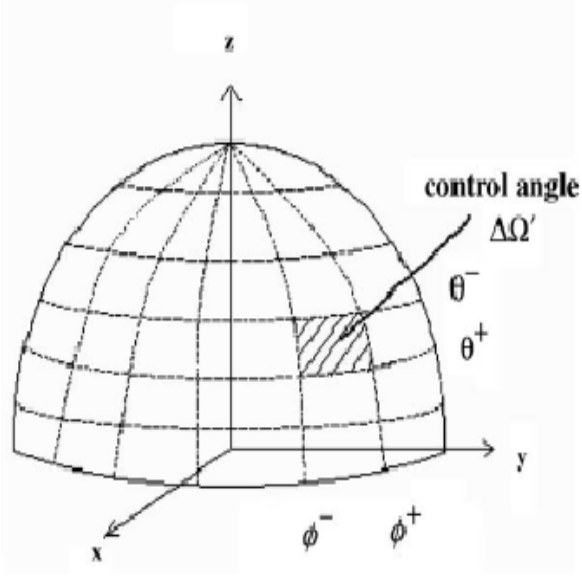

Fig 2.5 A typical control angle

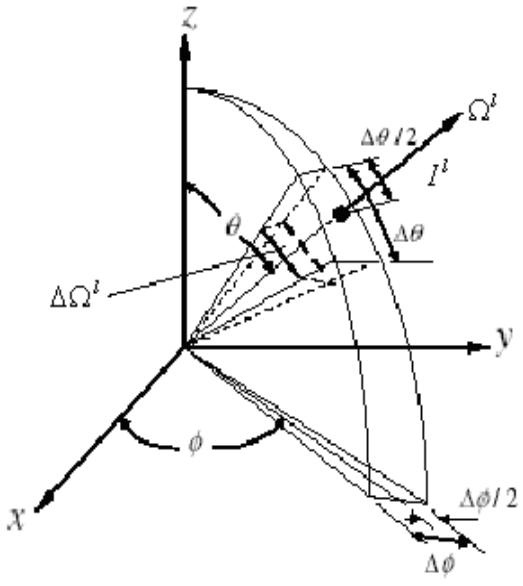

Fig 2.6 Intensity I^l in direction Ω^l in the center of the elemental sub-solid angle $\Delta\Omega^l$

CHAPTER 3

NUMERICAL METHODS

In this chapter, the numerical methods used in modeling the Transient Radiative Heat Transfer Equation are described. For modeling the TRT equation Finite Volume Method is used to discretize the governing equation then the overall positive variable treatment is applied to avoid any negative value of intensity in the final discretize equation. The finite volume method is described in section 3.1. Then the overall positive variable treatment is discussed in section 3.2. In section 3.3 solution procedure to get final value of nodal intensity through iterative process is discussed.

3.1 Finite Volume Method

In Finite Volume method, the domain is divided into a number of control volumes. The grid points are located at the center of control volume. This method is also called as control volume method since the conservation principles are applied to a fixed region in the control volume. The integral form of the conservation equation is integrated over each control volume to derive an algebraic equation with values of unknown variable (as for example I in the present problem). The discretization equation expresses the conservation principle for a finite control volume.

Typical two-dimensional Cartesian control volumes are shown in Fig. 3.1. The control volume interface is subdivided into four place faces for two-dimensional problem, which are denoted by lower case letters- *e*, *w*, *n*, and *s* corresponding to their direction along east, west, north and south respectively with respect to the central node *P*. Similarly, the adjacent control volume nodes are denoted by capital letters *E*, *W*, *N*, and *S* corresponding to their direction with respect to the central node *P*. There are various Radiation modeling technique like Monte Carlo method, Integral equation solution, Discrete transfer method, Discrete order method but in this study Finite Volume method is used because FVM yield more accurate result and this method is fully conservative.

3.2 Overall Positive Variable Treatment

The numerical method, overall positive variable treatment is used to avoid the occurrence of any negative value in the final discretized equation. In the previous chapter of mathematical formulation it can be seen in equation (36) in case of 1-D and in equation (61) in case of 2-D that in the final discretized equation negative values of coefficient is coming which can make the nodal intensity a negative value which is not possible at all because intensity cannot be negative. So to avoid this negative intensity it is necessary to make the equation such that it not yields a negative intensiy. So for the same reason overall positive variable treatment is applied.

so applying overall positive variable treatment in 1-D equation, the final equation with no negative variable is

$$\left[D_{cx}^{l}+\frac{D_{cx}^{l}}{I_P^{*}}\left(S_{ce^{+}}-S_{cw^{+}}\right)+\beta_{m,P}^{l}\Delta V\Delta\Omega^{l}\right]I_P^{l}=\left(\frac{\Delta V\Delta\Omega^{l}}{c\Delta t}\right)I_P^{l0}+D_{cx}^{l}I_W^{l}+D_{cx}^{l}\left(S_{pw^{+}}-S_{pe^{+}}\right)I_P^{*}+S_{m,P}^{l}\Delta V\Delta\Omega^{l} \tag{70}$$

Similarly applying the same for 2-D equation the equation become

$$\left[D_{cx}^{l}+\frac{D_{cx}^{l}}{I_P^{*}}\left(S_{ce^{+}}-S_{cw^{+}}\right)+D_{cy}^{l}+\frac{D_{cy}^{l}}{I_P^{*}}\left(S_{cn^{+}}-S_{cs^{+}}\right)+\beta_{m,P}^{l}\Delta V\Delta\Omega^{l}+\frac{\Delta V\Delta\Omega^{l}}{c\Delta t}\right]I_P^{l}=\left(\frac{\Delta V\Delta\Omega^{l}}{c\Delta t}\right)I_P^{l0}+D_{cx}^{l}I_W^{l}+D_{cx}^{l}\left(S_{pw^{+}}-S_{pe^{+}}\right)I_P^{*}+D_{cy}^{l}I_S^{l}+D_{cy}^{l}\left(S_{ps^{+}}-S_{pn^{+}}\right)I_P^{*}+S_{m,P}^{l}\Delta V\Delta\Omega^{l} \tag{71}$$

It can be seen in above two equations that after applying overall positive variable treatment the equation become free from any negative variable.

3.3 Overall Solution Procedure

The finite volume discretization results in a set of algebraic equations with the radiant intensities as the unknowns. An iterative method is used to solve the resulting set of algebraic equations within each time step. The solution process adopts a marching procedure to solve the set of equations.

The solution procedure is as follows:

1. Start with a suitable intensity distribution for the entire domain.

2. Proceed to the next time step.

3. Set the initial or the most current nodal intensities as the guessed values.

4. Update the upstream boundary intensities.

5. Following the marching order, calculate the nodal intensities for all internal control volume.

6. Calculate the radiation arriving and living the opposite walls.

7. Return to step 4 and repeat the calculation until convergence.

8. Stop when the desired time is reached or go to step 2 to advance to a new time step.

Now the above solution procedure is represented by the help of flowchart as shown in Fig (3.2).

In this chapter all the numerical methods which has been used to discretize the governing equation and to find the nodal intensity is discussed. In the next chapter the various result that are obtained by the use of discretized equation with certain boundary condition are presented.

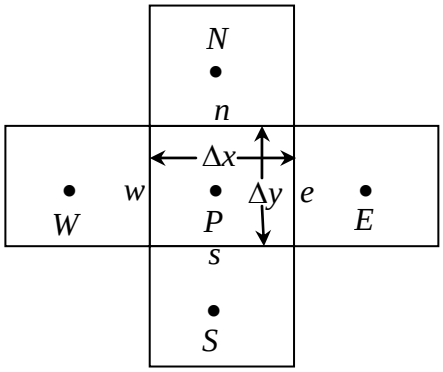

Figure 3.1 A typical two-dimensional control volume with specified notations

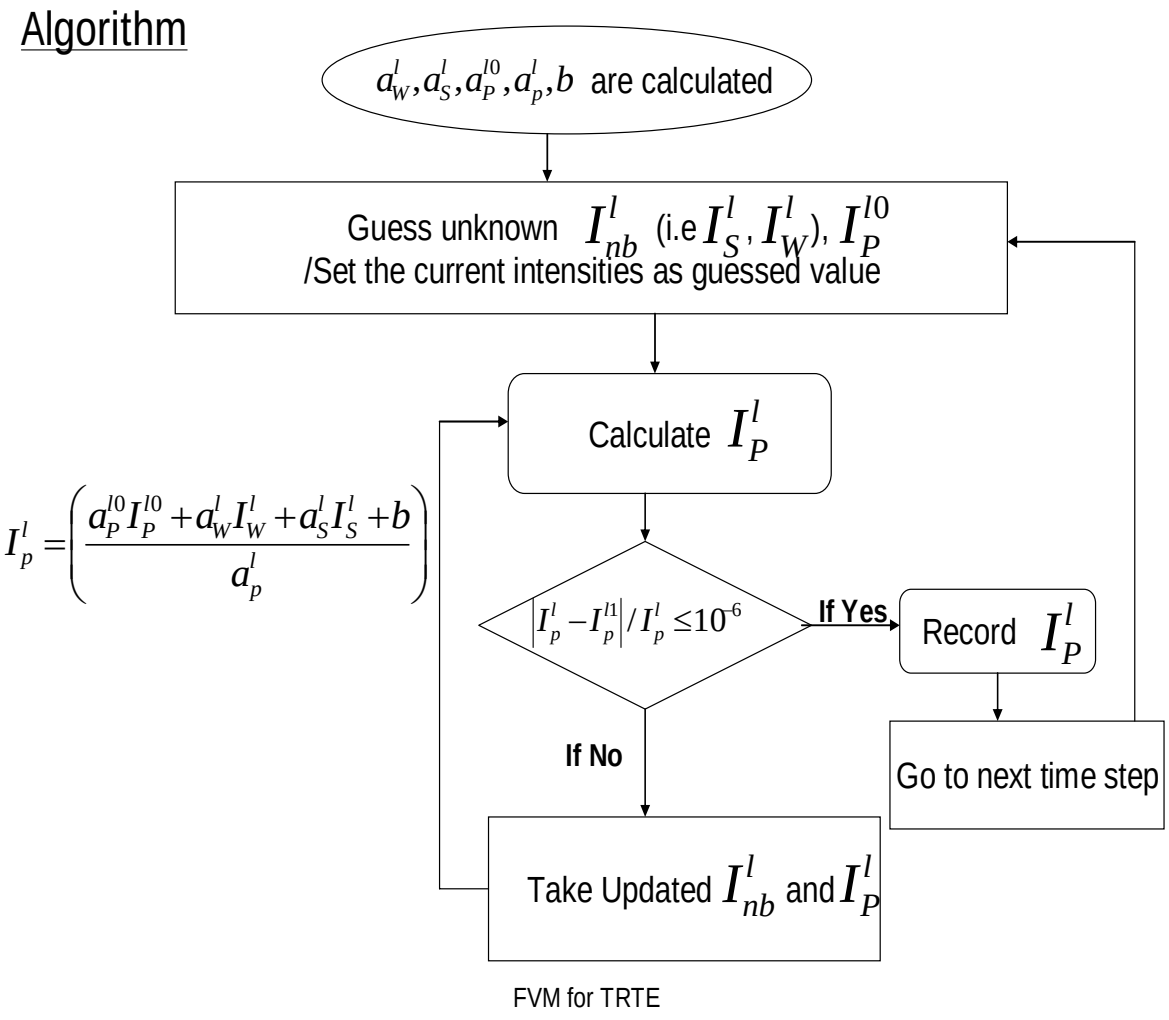

Figure 3.2 Flowchart of overall solution procedure

CHAPTER 4

RESULTS AND DISCUSSUION

In the present chapter, the various result that has been obtained by the help the above formulations and with the application of various numerical methods are discussed in detail.

The propagation of radiant energy in a two-dimensional slab consist of an absorbing-emitting medium maintained at a constant temperature with black, square enclosure subjected to diffuse radiation is examined. Result from the present procedure is compared with the result of Chai for steady state as shown in Fig (4.1) with calculation domain is discretized into 20×20 uniform control volume in the x and y direction and with angular discretization 2×8 control angles in θ and ϕ direction. With the same boundary condition and calculation domain for purely scattering medium has also been compared with the result of Chai for steady state and step scheme as shown in Fig (4.2) and found that both the graph are overlapping. The present procedure is then used to model other situation.

A grid independent test was done with different spatial and angular grid size. It is observed that further refinement to the grid size of 40×40 control volume and 8×4 control angles results in negligible change in the results as seen in Fig (4.3) and Fig (4.4). Henceforth the above grid size is used for further presentation of result.

The comparison of step and CLAM scheme is shown in Fig (4.5). After comparing the steady result shown in Fig (4.1) and Fig (4.2) the problem involved the transient term as well with same boundary condition as described above. Both step and CLAM scheme are compared in Fig (4.5) and it shows that how the transient behavior of the problem considered changes to steady state after infinite time step. This steady state graph obtained from transient equation is similar to that obtained from steady equation. In this graph the wall heat flux for various time steps is plotted for both scheme and shows that after each time step the value of net flux increases to certain value and become constant after certain time step which is similar to the steady state net flux at the wall.

In Fig (4.6) medium flux is shown for the above problem using CLAM scheme. It is clearly visible in the graph that the value of flux is very small at the center and increases as we move towards wall. The flux at the center give small value because the value of the incoming flux i.e. the flux that comes from the wall towards center increases as it moves toward center and

minimizing the value of outgoing flux, because of this reason the value of flux is small at the center and increases as it moves towards wall in any direction and it can be seen from Fig (4.6). It has been explained earlier that the value of flux is maximum at the wall because at wall there is no flux in opposite direction to minimize the effect of outgoing flux.

Figure (4.7) and Fig (4.8) shows the flux with grey wall with different value of emissivity. The top and bottom wall are made grey by giving emissivity value less than one to this walls. The value of flux for top and bottom walls is then calculated for different value of emissivity. The variation in flux on top and bottom wall with change in emissivity is shown in Fig (4.7). It is clear from the graph that the net flux decreases as the value of emissivity decreases, this is because as emissivity decreases reflectivity of the wall increases and makes the net flux to decreases. The net flux is maximum for black wall with emissivity equal to one which is shown in graph. For the same case as above with top and bottom wall grey, the side wall flux are plotted for different value of emissivity as shown in Fig (4.8). It is clear from the graph that by making top and bottom wall grey it not make much difference in the value of side wall flux because side wall are still black.

The effect of scattering albedo in the net flux is shown in Fig (4.9). In all the above calculation purely isothermal with absorbing-emitting medium is plotted with scattering coefficient is equal to zero. Now by considering the scattering coefficient together with absorption coefficient graph is plotted for different value of scattering albedo. It can be seen from the graph that as the value of omega increases the net flux decreases it is because as scattering is increases the flux that was reaching to the wall previously when scattering is zero now scatters in other directions also and due to this reason the complete flux not reaches to the wall of the domain and the net flux at wall decreases.

Figure (4.10) shows the effect of optical thickness on wall flux when scattering albedo remain constant. It is clear from the graph that as the value of optical thickness increases the net flux at the wall also increases. Optical thickness increasing means the size of the domain increasing and it has been already seen that as we move from center towards the wall net flux increases, it means that as the size of the domain increases the distance between the centre and wall also increases, so the flux that is reaching to the wall also increases because it is know travelling

longer path so getting more flux added in the direction of travel and hence the net flux at the wall increases.

Transient evolution of radiative transfer in one-dimensional medium is examined. The walls are diffuse and black and at a cold temperature (0 K), at time t = 0, the temperature of the bottom boundary (Z=0) is suddenly raised to provide an emissive power of π for all subsequent of time. The medium scatters radiation isotropically with an optical thickness and scattering albedo of 1 and 0.5, respectively. Forty (40 polar and 1 azimuthal) control angles are used to discretize the angular space. The spatial domain is discretized into 300 uniform control volumes. Fig (4.11) and Fig (4.12) shows the comparison of present result with the result of Chai for radiative flux and incident radiation for non dimensional time step equal to 60. It can be seen that both the graph are overlapping and this is further modify to get the effect of anisotropicity in Fig (4.13) and Fig (4.14). It can be seen from the Fig (4.13) that the value of flux in forward scattering is more than backward scattering, it is because as we move form bottom to top, scattering is more in that direction and get accumulated in that direction and due to cumulative effect of that forward scattering increases and backward scattering is in the opposite direction is less (can be seen from Fig 4.14) than previous because scatter is less in backward direction. Fig (4.15) shows the effect of anisotropic scattering in irradiation, it is clear from the graph that anisotropic scattering not make much effect on the irradiation.

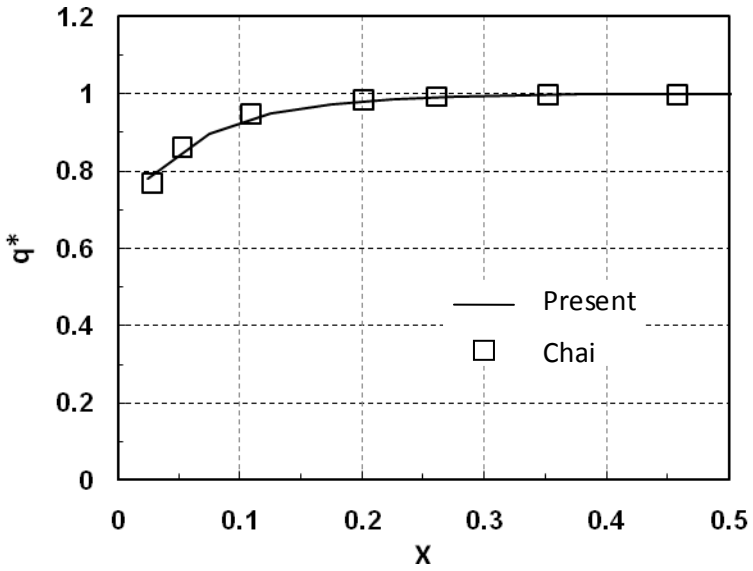

Figure 4.1 Comparison for isothermal emitting absorbing medium

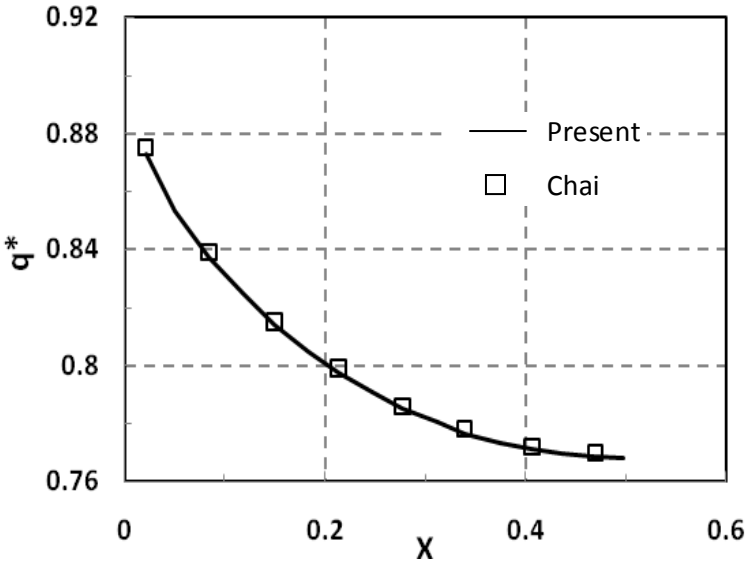

Figure 4.2 Comparison for purely scattering medium

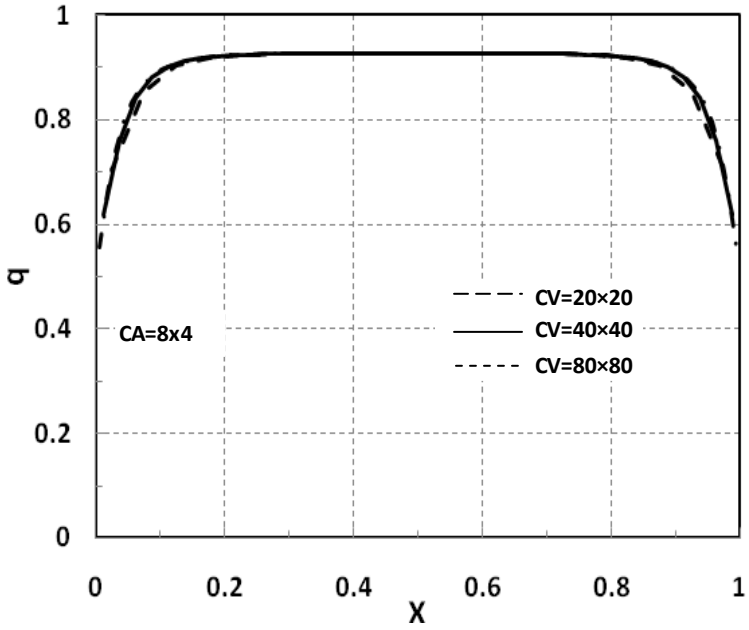

Figure 4.3 Grid independent test for control volume

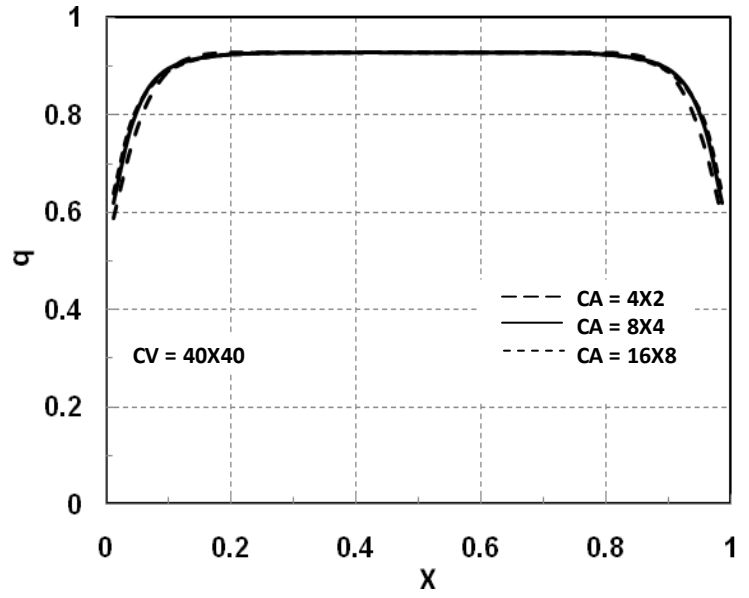

Figure 4.4 Grid independent test for control angle

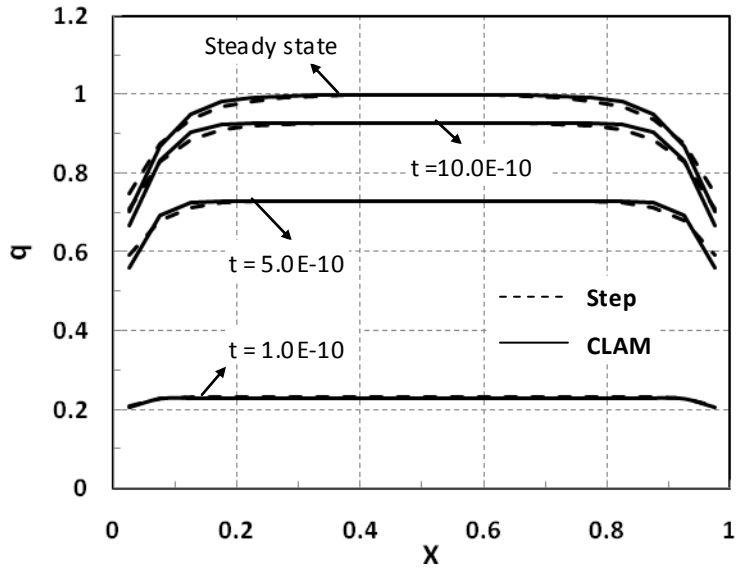

Figure 4.5 Comparison of Step and CLAM scheme for transient state

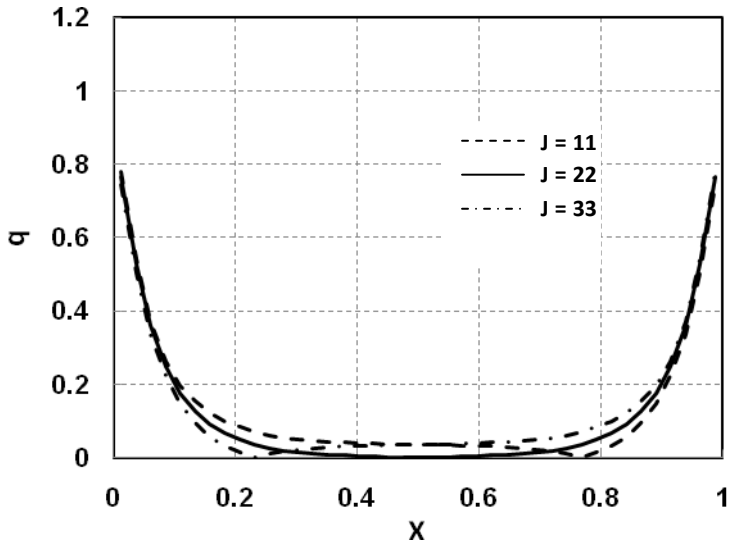

Figure 4.6 Medium flux for different location in y-direction

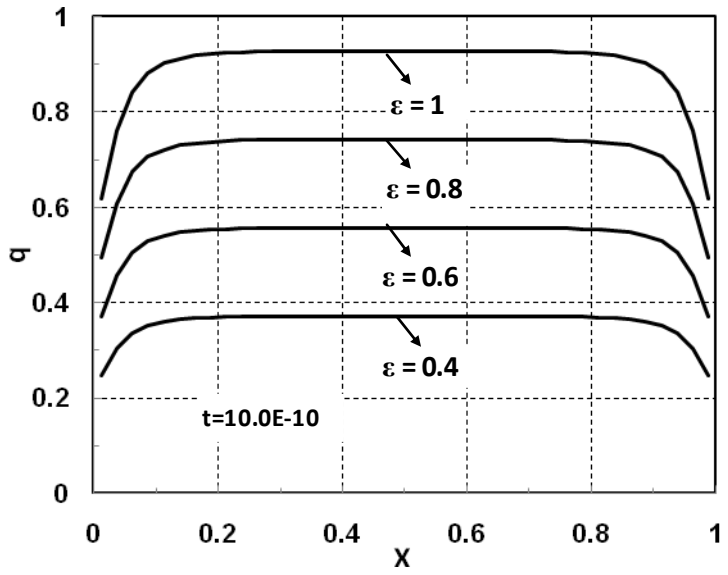

Figure 4.7 Top and bottom wall flux with both both top and bottom wall grey

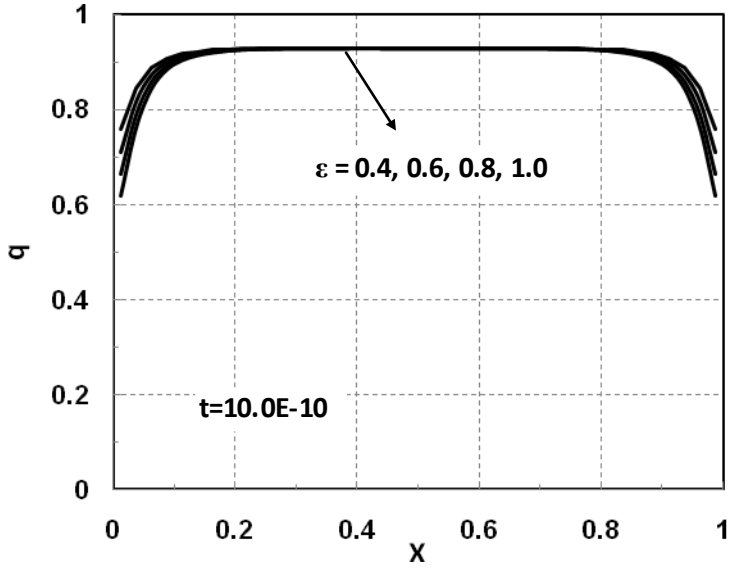

Figure 4.8 Left and right wall flux with top and bottom wall grey

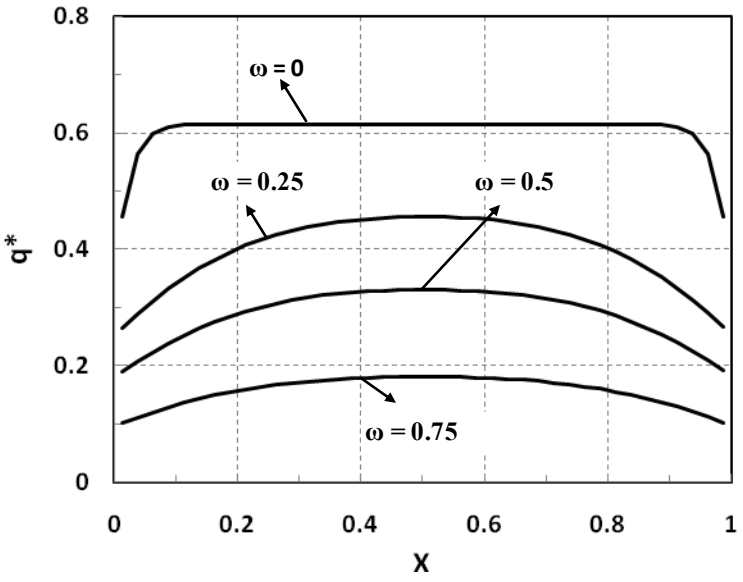

Figure 4.9 Effect of scattering albedo on wall flux

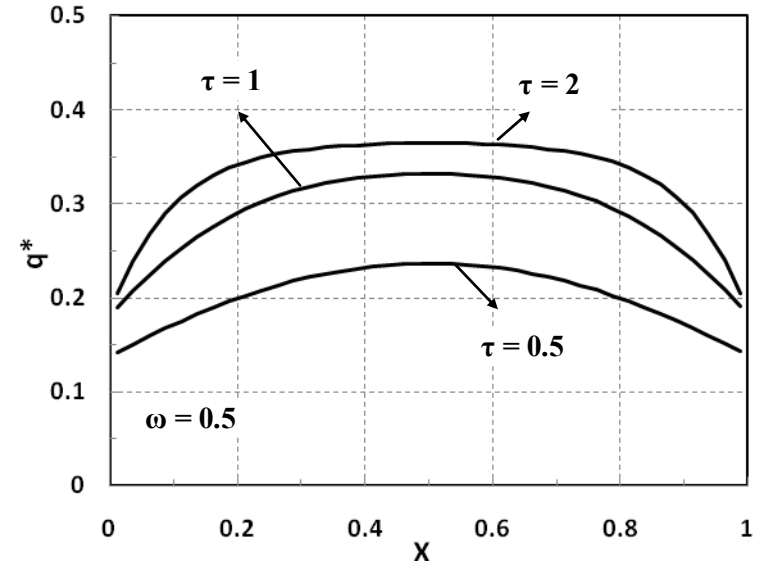

Figure 4.10 Effect of optical thickness on wall flux

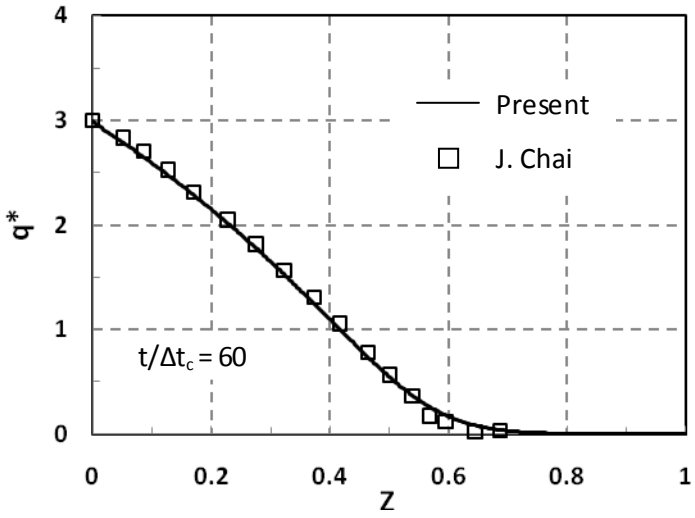

Figure 4.11 Comparison for isotropic scattering

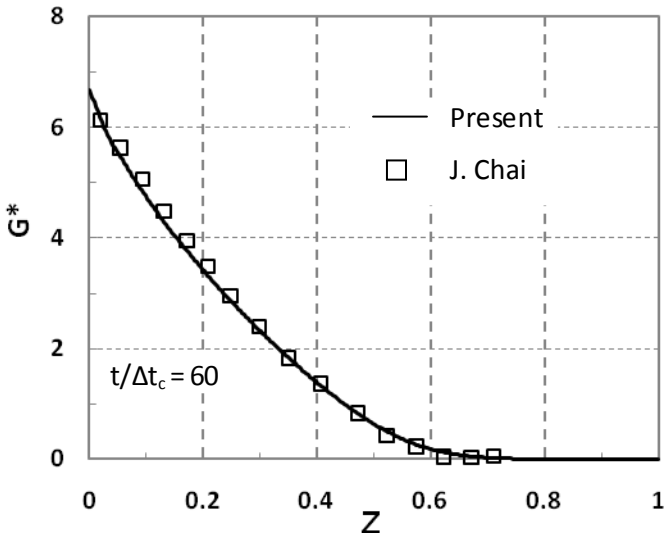

Figure 4.12 Comparison of irradiation for isotropic scattering

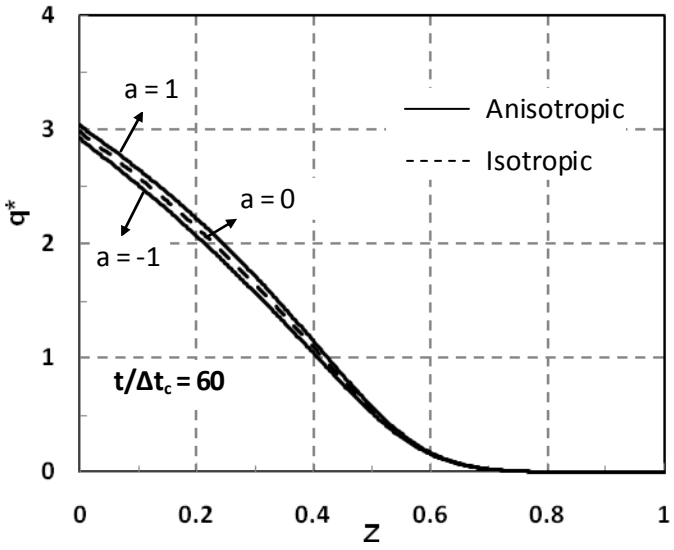

Figure 4.13 Wall flux for anisotropic scattering

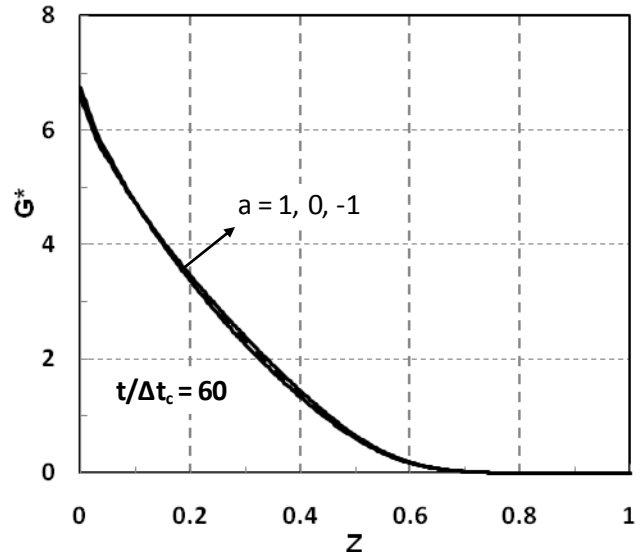

Figure 4.14 Irradiation for anisotropic scattering

CHAPTER *5*

CONCLUSION

5.1 Conclusion

- ✓ Fundamental understanding and unique features of transient radiation together with its behavior in participating medium is studied.
- ✓ Finite Volume Formulation for 1-D and 2-D model has been done.
- ✓ The effect of anisotropic scattering in 1-D model has been studied
- ✓ Comparison of both the scheme has been done and it is found that ClAM scheme is giving better result than Step scheme.
- ✓ Effect of various parameter (emissivity, scattering albedo, optical thickness) on wall flux has been studied.
- ✓ All the above formulation and comparison is done considering transient behavior of radiative transfer equation.

5.2 Scope for future work

The present work can be further extended to solve the following problem.

- ✓ All the formulation that has been done is for purely radiative mode of heat transfer, it can be extended for combined conductive and radiative mode of heat transfer.
- ✓ The present problem can be extended to collimated Radiation for both 1-D and 2-D model.
- ✓ In the present work effect of anisotropic scattering for 1-D model has been discussed. The same can be extended for 2-D model.
- ✓ In the present work, the problem is solved using two scheme. The work can also be extended for another high order spatial differential scheme i.e. SMART scheme.
- ✓ In the present work, transient radiative problem for homogeneous medium and regular geometry is discussed. It can be extended to inhomogenous medium and complex geometry like cylindrical and L shaped body.

REFERENCES

[1] Beach H. L., Ozisik M. N. and Siewert C. E., Radiative transfer in linearly anisotropic-scattering, conservative and non-conservative slabs with reflective boundaries, Int. Jl. Heat and Mass Transfer, 14(1971)1551-1565.

[2] Modest M.F., "Radiative heat transfer". McGraw Hill International Edition, 1996

[3] Mitra K, Kumar S, Microscale aspects of thermal radiation transport and laser application, Adv Heat Transfer, 33(1999)187-294.

[4] Mitra K, Kumar S, Development and Comparison of models for light-pulse transport through scattering–absorbing media, Applied Optics, 38(1999)188-196.

[5] Guo Z., Kumar S., San K-C., "Multidimensional Monte Carlo simulation of short pulse transport in scattering media". Jl. Of Thermophysics Heat Transfer, 14, 4(2000)504-511.

[6] Guo Z., Kumar S., "Discrete-ordinate solution of short-pulsed laser transport in two-dimensionl turbid media". Appl. Opt 40(19) (2001)3156-63.

[7] Guo Z., Maruyama S., "Radiative heat transfer in inhomogeneous, non-gray and anisotropically scattering media". International Journal of Heat and Mass Transfer 43(2000) 2325-2336.

[8] Sakami M, Mitra K, Hsu P F., "Analysis of light-pulse transport through two-dimensional scattering and absorbing media". Journal of Quantitative Spectroscopy & Radiative Transfer 73 (2002) 169–179.

[9] Mitra K., Lai M.S., Kumar S., "Transient radiation transport in participating media within a rectangular enclosure". AIAA J Thermophysics Heat Transfer; 11, 3(1997)409-14.

[10] Hsu P F, Effects Of multiple Scattering and reflective boundary on the transient radiative transfer process. Int. J. Therm. Sci., 40(2001)539–549.

[11] Lu X., Hsu P-f, "Reverse Monte Carlo method for transient radiative transfer in participating media". ASME Journal of Heat Transfer, 126(2004) 621-627.

[12] Wu C.Y, Wu S.H., Integral equation formulation for transient radiative transfer in an anisotropically scattering medium, Int. J. Heat Mass Transfer, 122(2000)2009-2020.

[13] Tan Z.M., Hsu P.F., An integral formulation of transient radiative transfer, J. Heat Transfer, 123(2001)466–475.

[14] Guo Z, Kumar S, Radiation element method for transient hyperbolic radiative transfer in plane-parallel inhomogeneous media, Numerical Heat Transfer, Part B, 39(2001)371-387.

[15] Hasegawa Y., Yamada Tamura Y., M., Nomura Y., "Monte Carlo simulation of light transmission through living tissues". Applied Optics 30(1991)4515-4520.]

[16] Brewster M.Q., Yamada Y., “Optical properties of thick, turbid media from picosecond time resolved light scattering measurements”. International Journal of Heat and Mass Transfer 38(1995)2569-2581.

[17] Chai J.C., Lee H.S, Patankar S.V., “Finite Volume Method for radiation heat transfer”. Jl. Of Thermophysics Heat Transfer, 8, 3(1994)419-425.

[18] Chai J.C, One-dimensional transient radiative heat transfer modeling using a finite volume method, Numer. Heat Transfer B, 44(2003)187–208.

[19] Chai J C, Transient radiative transfer in irregular two-dimensional geometries, Journal of Quantitative Spectroscopy & Radiative Transfer, 84(2004)281-294.

[20] Coelho P.J, Bounded skew high order resolution schemes for the discrete ordinates method, Journal of Computational physics, 175(2002)412-437.

[21] Rath P, Mishra S.C, Mahanta P, Saha U.K, Mitra K, Discrete transfer method applied to transient radiative problems in participating medium, Numer. Heat Transfer A, 44(2003)183–197.

[22] Sarma D.J, Mishra S.C, Mahanta P, Analysis of collimated radiation using the discrete transfer method, J. Quant. Spectrosc. Radiat. Transfer, 96(2005) 123–135.

[23] Okutucu T, Yener Y, Radiative transfer in participating media with collimated short-pulse Gaussian irradiation, J. Phys. D: Appl. Phys, 39(2006)1976–1983.

[24] Muthukumaran R, Mishra S C, Transient response of a planar participating medium subjected to a train of short-pulse radiation, International Journal of Heat and Mass Transfer, 51(2008)2418–2432.

[25] An W., Ruan L.M., Tan H.P., Qi H., “Least square finite element analysis for transient radiative transfer in absorbing and scattering media”. ASME Journal of Heat Transfer, 128(2006) 499-503.

[26] An W., Ruan L.M., Tan H.P., Qi H., Leo Y.M., “Finite element simulation for short pulse light radiative transfer in homogeneous and non-homogeneous media”. ASME Journal of Heat Transfer, 129(2007) 353-362.

[27] Yilmazer A, Kocar C, Ultraspherical-Polynomials approximation to the radiative heat transfer in a slab with reflective boundaries, International Journal of Thermal Sciences, 47(2008)112–125.

[28] Sakami M., Mitra K., and Hsu P. F., Transient Radiative Transfer in Anisotropically Scattering Media Using Monotonicity-Preserving Schemes, 2000 Int. Mechanical Engineering Congress and Exposition, November 5–10, 2000, Orlando, FL, USA.